Oncostatin M promotes the osteogenic differentiation of mouse MC3T3-E1osteoblasts through the regulation of monocyte chemotactic protein-1

WENBIAO ZHENG and JUNHUI GUAN

Department of Orthopedics, Taizhou Municipal Hospital, Taizhou, Zhejiang 318000, P.R. China

Received August 24, 2017; Accepted December 12, 2017

DOI: 10.3892/mmr.2018.9261

Abstract. The present study investigated the function of oncostatin M (OSM), which may be associated with monocyte chemotactic protein-1 (MCP-1), on mouse MC3T3-E1 osteoblast development and bone remodeling. Levels of MCP-1, macrophage inflammatory protein 1α (MIP1α) and regulated upon activation normal T cell expressed and secreted (RANTES) were measured by ELISA. Cell viability, migration and invasion abilities were detected by MTT, wound healing and Transwell assays, respectively. Western blotting was performed to detect levels of phosphorylated protein kinase B (Akt). Reverse transcription-quantitative polymerase chain reaction and western blotting were performed to detect the levels of matrix metalloproteinases (MMP)-1, -2 and -3. The results demonstrated that OSM treatment significantly increased MCP-1 levels in a dose-dependent manner. Interleukin (IL)-1, also significantly increased MCP-1 levels; however, treatment with other cytokines, including IL-6, IL-11 and leukemia inhibitory factor did not affect MCP-1 levels to the same extent. In addition, OSM did not affect levels of the chemokines MIP1α and RANTES; indeed, only IL-1 significantly increased levels of MIP1α and RANTES. OSM treatment promoted the proliferation, migration and invasion in a dose-dependent manner, which were inhibited by MCP-1 silencing. The expression of phosphorylated-Akt, MMP-1, -2 and -3 were increased by OSM treatment; however, these increases were reversed following MCP-1 silencing. Collectively these data suggest that OSM promotes the differentiation of mouse MC3T3-E1 osteoblasts via regulation of MCP-1 expression. These results may therefore provide novel insights into bone repair and remodeling.

Correspondence to: Dr Junhui Guan, Department of Orthopedics, Taizhou Municipal Hospital, 381 Zhongshan East Road, Shujiang, Taizhou, Zhejiang 318000, P.R. China
E-mail: junhuiguan_jhg@163.com

Key words: oncostatin M, osteogenic differentiation, osteoblasts, monocyte chemotactic protein-1

Introduction

Skeletal repair and remodeling help to maintain bone integrity and this process occurs over the life course. It clears away aged bone tissues, in addition to repairing bone injuries and fractures (1). The remodeling process involves two mechanisms: Bone resorption by osteoclasts and bone formation by osteoblasts (2). These mechanisms are tightly coordinated to ensure that skeletal integrity is maintained; the dysregulation of bone remodeling may lead to the onset of bone diseases, including osteoarthritis and osteoporosis (3).

Cytokines and chemokines are usually secreted by immune cells, which serve critical roles in host defense systems and help to ensure that tissues remain in a healthy state (4). Studies have already determined the roles that chemokines in the immune system (5,6). However, the effect on bone remodeling requires further research. Certain chemokines, including TNFα, IL-6 and RANKL, are able to regulate osteoblasts and osteoclasts (7-10). Oncostatin M (OSM) is a cytokine which is part of the interleukin (IL)-6 family and originates from monocytes, macrophages or T-cells that are involved in chronic inflammation (11). OSM is commonly associated with osteoblast proliferation and collagen synthesis and is able to stimulate bone formation and resorption (12,13). It also serves a number of functions in skeletal tissue alteration, bone metabolism and inflammatory diseases (14,15). Furthermore, OSM assists with inducing the expression of monocyte chemotactic protein-1 (MCP-1) in human proximal tubular cells, human aortic adventitial fibroblasts and smooth muscle cells (16,17).

MCP-1 [also known as C-C motif chemokine (CCL)2], macrophage inflammatory protein 1α (MIP1α, also known as CCL3) and regulated upon activation normal T cell expressed and secreted (RANTES, also known as CCL5) are members of the CC subfamily of chemokines that contain conserved cysteine residues (18,19). MCP-1induces the recruitment and activation of leukocytes to alleviate acute inflammation (20). During bone remodeling, MCP-1 is secreted by osteoblasts and promotes osteoclast differentiation to stimulate matrix metalloproteinase (MMP)-induced cell fusion (21).

The different types of MMPs include MMP-1 (fibroblast collagenase), MMP-2 (gelatinase A) and MMP-3 (stromelysin-1) (22). MMPs are primarily distributed in the bone matrix and usually regulate the proteolysis of extracellular matrix structural proteins, as well as induce cell metastasis (23). MMPs

also participate in bone repair and remodeling (24). MMPs are secreted by chondrocytes and synovial lining cells and elevated MMPs have been detected in the synovial joints of patients with rheumatoid arthritis (25,26). The cytokine IL-1is able to promote MMP-1 and MMP-3 expression in synovial tissues (27) and MMP-2 mediates sarcomere degeneration during OSM-induced cardiomyocyte dedifferentiation and regeneration (28). Furthermore, OSM is able to promote trophoblast invasion activity by stimulating the activity of MMP-2 and MMP-9 (29).

To the best of the authors' knowledge, the mechanism by which OSM stimulates MCP-1 in osteoblasts, including during its regulation of MMPs, remains to be elucidated. Therefore, the present study aimed to determine the regulatory function of OSM in parallel with MCP-1 in the skeletal repair and remodeling process, in order to provide novel insights into bone health.

Materials and methods

Cell culture. Mouse MC3T3-E1 osteoblasts were purchased from the American Type Culture Collection (Manassas, VA, USA). Osteoblasts were cultured in Dulbecco's Modified Eagle's medium (Gibco; Thermo Fisher Scientific, Inc., Waltham, MA, USA) containing 10% fetal bovine serum (FBS; Gibco; Thermo Fisher Scientific, Inc.) and 1% penicillin/streptomycin (Invitrogen; Thermo Fisher Scientific, Inc.) in 5% CO_2 at 37˚C. For subsequent experiments, cells in the logarithmic growth phase were used.

ELISA. Cells were cultured in 12-well plates and stimulated with varying concentrations of OSM (0, 1, 5, 10, 30 and 50 ng/ml), IL-1 (10 ng/ml), IL-6 (30 ng/ml), leukemia inhibitory factor (LIF; 20 ng/ml) or IL-11 (30 ng/ml) for 24 h. All cytokines were purchased from R&D Systems, Inc. (Minneapolis, MN, USA). Cells were centrifuged at 6,000 x g and 4˚C for 10 min, and supernatants were collected and stored at -20˚C prior to analysis.

MCP-1, MIP1α and RANTES levels were respectively determined using the Mouse CCL2/JE/MCP-1 Quantikine ELISA kit (MJE00; R&D Systems, Inc.), Mouse CCL3/MIP1α Quantikine ELISA kit (MMA00; R&D Systems, Inc.), and Mouse/Rat CCL5/RANTES Quantikine ELISA kit (MMR00; R&D Systems, Inc.), following the manufacturer's protocol. Cell supernatants (50 μl) or specific standard substances (MCP-1, MIP1α and RANTES) from the kits were added to the wells of a 96-well plate and incubated for 2 h at room temperature. Biotinylated conjugates from the kits were added to the wells and incubated for 2 h at room temperature. Following rinsing, the substrate avidin peroxidase complex was added and incubated for another 30 min. Reactions were attenuated using stop solution and optical density values were measured at a wavelength of 450 nm using a microplate reader. The concentration of cytokines in samples was calculated via interpolation of a standard curve.

MTT assay. Cell viability was measured by MTT assay. Cells were seeded into a 96-well plate at $5x10^3$ cells/well and stimulated using different concentrations of OSM (10, 30 and 50 ng/ml) for 24 h. Subsequently, 10 μl MTT reagent was added to each well, the formazan crystals dissolved by dimethyl sulfoxide, and the absorbance was measured at a wavelength of 570 nm, following the manufacturer's protocol (Cell Growth Detection kit MTT-Based; Sigma-Aldrich; Merck KGaA, Darmstadt, Germany).

Wound healing assay. Cells were seeded in 12-well plates at $1x10^5$ cells/well and stimulated by different concentrations of OSM (10, 30 and 50 ng/ml). The confluent monolayer of cells was scratched gently using a pipette yellow tip to form a cell-free area in wells. Cells were observed using a light microscope (magnification, x200) 24 h after stimulation.

Cell invasion assay. Cell invasion was detected using 24-well Transwell chambers containing 8-μm pore polycarbonate filters (Corning Incorporated, Corning, NY, USA) and chambers pre-coated with Matrigel (BD Biosciences, San Jose, CA, USA). Briefly, cells treated with different concentrations of OSM (10, 30 and 50 ng/ml) for 24 h were collected and transferred to the upper chambers ($5x10^4$ cells/well) containing DMEM (Gibco; Thermo Fisher Scientific, Inc.) and Matrigel. The bottom chambers contained DMEM culture medium (Gibco; Thermo Fisher Scientific, Inc.) and 10% FBS. Following incubation for 24 h, invaded cells on the lower surface that passed through the filter were fixed with ice cold methanol for 30 min and stained with 0.1% crystal violet for 30 min at 37˚C. Invaded cells were counted in four randomly selected high-power fields using a light microscope (magnification, x200) and the relative number of cells was calculated. Experiments were repeated 3 times and the average of the 3 independent experiments was recorded.

Small interfering (si)RNA transfection. MCP-1 siRNA transfection was performed to determine whether the effect of OSM on cell proliferation and invasion is dependent on MCP-1 expression. siRNA-MCP-1 was designed and synthesized by Shanghai GenePharma Co., Ltd. (Shanghai, China) as 5'-AACTTCACC AATAGGAAGATC-3'. A nonspecific sequence was used as NC control: 5'-CACATTTCAAACGTAGTAGAA-3'. For siRNA transfection, cells were seeded into 12-well plates at a concentration of $5x10^4$ cells/well and 50% confluent cells were transfected with 5 nmol/l MCP-1 siRNA (siMCP-1 group) or nonspecific siRNA (mock group), with HiPerFect Transfection Reagent (Qiagen GmbH, Hilden, Germany) for 24 h, according to the manufacturer's protocol. Then cells were stimulated with OSM (30 ng/ml) for 24 h, in the OSM+siMCP-1 group or OSM+mock group respectively. Cells that did not receive any treatment, including transfection and OSM stimulation, were used as a control (Control group). Only cells stimulated with 30 ng/ml OSM were defined as OSM group. Subsequently, reverse transcription-quantitative polymerase chain reaction (RT-qPCR) and western blotting were conducted to determine the interference efficiency by measuring MCP-1 levels in the OSM+siMCP-1, OSM+mock, OSM and control groups.

RT-qPCR. Levels of mRNA were measured using RT-qPCR. Total RNA was extracted from cells using an RNeasy kit (Qiagen GmbH) and cDNA was synthesized with 1 μg total RNA using an EN-QuantiTect Reverse Transcription kit (Qiagen GmbH), according to the manufacturer's protocol. qPCR was performed using Fast SYBR Green Master mix (Applied Biosystems; Thermo Fisher Scientific, Inc.) on a ABI 7300 Thermocycler (Applied Biosystems; Thermo Fisher Scientific, Inc.). The reactions were conducted for 15 sec

Table I. Primers used in the reverse transcription-quantitative polymerase chain reaction.

Name	Type	Sequence (5'-3')
MCP-1	Forward	CCACTCACCTGCTGCTACTC
	Reverse	AAGGCATCACAGTCCGAGTC
MMP-1	Forward	GTTGCGGCTCATGAATTGGG
	Reverse	TTGGCTGGTTGGGATTCTGG
MMP-2	Forward	AGGATACCCCAAGCCACTGA
	Reverse	CCTGGTGTGCAGCGATGAAG
MMP-3	Forward	ATGGAACTCCCACAGCATCC
	Reverse	TGCCCTCGTATAGCCCAGAA
GAPDH	Forward	GGTTGTCTCCTGCGACTTCA
	Reverse	CCCTAGGCCCCTCCTGTTAT

MCP-1, monocyte chemotactic protein-1; MMP, matrix metalloproteinase.

at 95˚C for pre-heating, followed by 40 cycles of denaturation at 95˚C for 15 sec and annealing/extension at 60˚C for 25 sec, and a final step of 72˚C for 10 min. The primer sequences used are presented in Table I. GAPDH was used as a reference gene. The quantification was identified by $2^{-\Delta\Delta Cq}$ method (30).

Western blot analysis. Cells were lysed by protein lysis reagent P0013 (Beyotime Institute of Biotechnology, Haimen, China), and cell lysis was centrifuged at 12,000 x g for 10 min at 4˚C. The supernatants were collected and the protein concentrations were determined using a bicinchoninic acid assay (Beyotime Institute of Biotechnology, Haimen, China). Subsequently, proteins (20 μg/lane) were electrophoresed using 15% SDS-PAGE and electroblotted onto a polyvinylidene fluoride (PVDF) membrane (EMD Millipore, Billerica, MA, USA). Following blocking with 5% nonfat dry milk in PBS for 1 h at 37˚C, membranes were incubated overnight at 4˚C with specific primary antibodies. GAPDH was used as a loading control. The primary antibodies were: Rabbit anti-MCP-1 (ab25124; 1:2,000), anti-p-AKT (ab38449; 1:1,000), anti-Akt (ab8805; 1:500), anti-MMP-1 (ab137332, 1:2,000), anti-MMP-2 (ab37150; 1:1,000), anti-MMP-3 (ab53015; 1:1,000) and anti-GAPDH (ab9485; 1:2,500). Membranes were then probed with horseradish peroxidase-conjugated secondary antibodies: Goat anti-rabbit IgG H&L (HRP; ab6721; 1:5,000) at 37˚C for 1 h. The PVDF membrane was exposed to an X-ray film and immunoreactive bands were detected using enhanced chemiluminescence detection reagents (GE Healthcare, Chicago, IL, USA). Band densities were quantified using Bio-Rad ChemiDoc™ XRS+System with Image Lab™ software version 4.1 (Bio-Rad Laboratories, Inc.). All antibodies were purchased from Abcam (Cambridge, UK).

Statistical analysis. All values were expressed as mean ± standard deviation of 5 independent experiments. Statistical analysis was conducted using SPSS version 13.0 statistical software (SPSS, Inc., Chicago, IL, USA) and significance was determined by performing one-way analysis of variance followed by Dunnett's post hoc test. $P<0.05$ was considered to indicate a statistically significant difference.

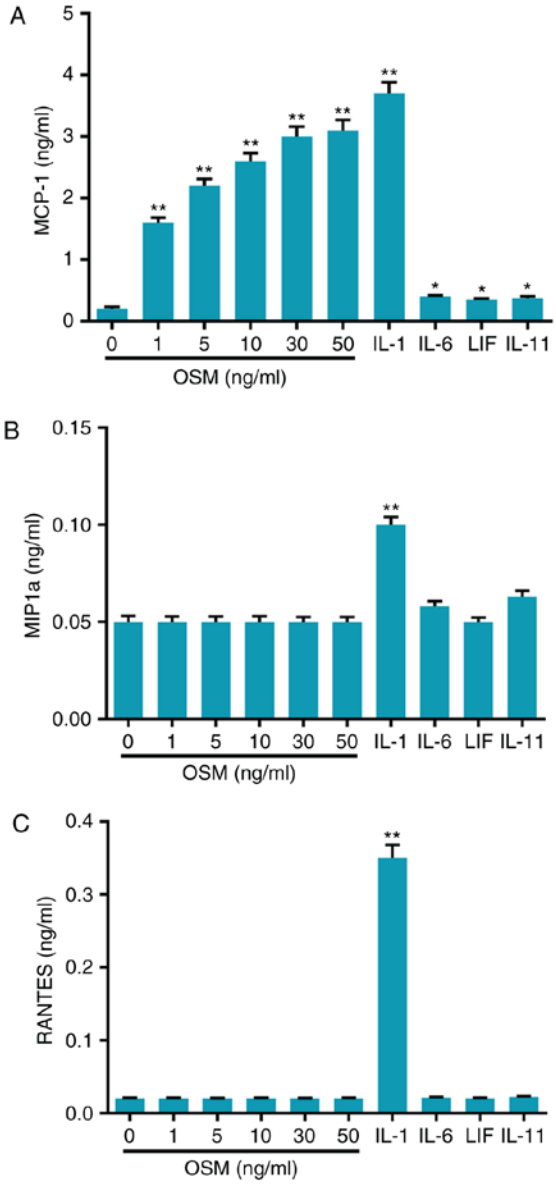

Figure 1. OSM stimulated chemokine expression in osteoblasts. Cells were stimulated with cytokines, including OSM (0, 1, 5, 10, 30 and 50 ng/ml), IL-1 (10 ng/ml), IL-6 (30 ng/ml), LIF (20 ng/ml) and IL-11 (30 ng/ml). Supernatants were collected and analyzed using ELISA to determine levels of (A) MCP-1, (B) MIP1α and (C) RANTES. Data are presented as the mean ± standard deviation. n=5. *P<0.01 and **P<0.01 vs. control. OSM, oncostatin M; IL, interleukin; LIF, leukemia inhibitory factor; MCP-1, monocyte chemotactic protein-1; MIP1α, macrophage inflammatory protein 1α; RANTES, regulated upon activation normal T cell expressed and secreted.

Results

The effect of the cytokines OSM, IL-1, IL-6, LIF and IL-11 on the chemokines MCP-1, MIP1α and RANTES in osteoblasts. ELISA was performed to assess the responses of cells to OSM, IL-1, IL-6, LIF and IL-11. Cells were stimulated with OSM (0, 1, 5, 10, 30 and 50 ng/ml), IL-1 (10 ng/ml), IL-6 (30 ng/ml), LIF (20 ng/ml) and IL-11 (30 ng/ml). Supernatants were collected and the levels of MCP-1, MIP1α and RANTES were analyzed using ELISA. The results revealed that IL-1

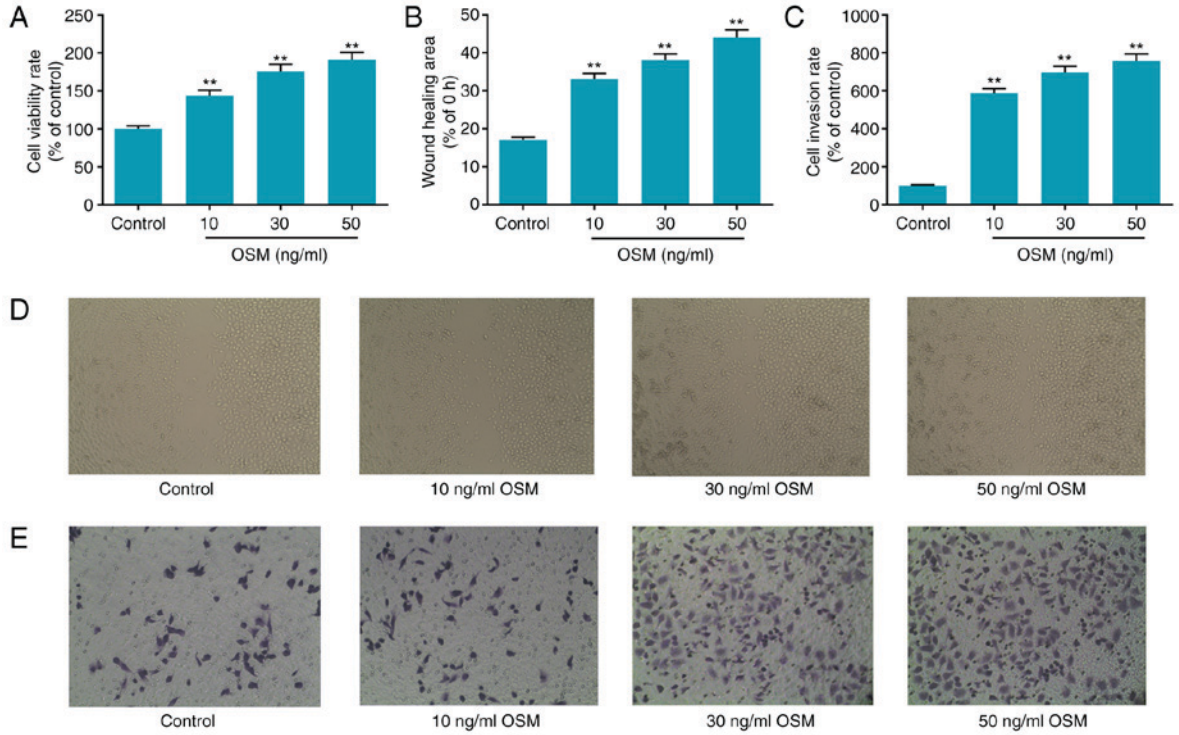

Figure 2. OSM induced cell progression in osteoblasts. (A) An MTT assay was performed to detect cell viability and cells were counted 24 h following stimulation with different concentrations of OSM (10, 30 and 50 ng/ml). (B) Cell migration abilities were measured using a wound healing assay 24 h after scratch. (C) Cell invasion abilities were evaluated using a Transwell invasion assay and cells were counted after 24 h incubation. (D) Images of wound healing assay and (E) Transwell invasion assay, magnification x 200. Data were presented as mean ± standard deviation n=5. **P<0.01 vs. control. OSM, oncostatin M.

significantly increased levels of the cytokines MCP-1, MIP1α and RANTES compared with controls (all P<0.01; Fig. 1A-C). Furthermore, IL-6, LIF and IL-11 significantly increased levels of MCP-1, and did not affect expression levels of MIP1α and RANTES, compared with the control (Fig. 1B and C). In addition, the concentrations of MCP-1 significantly increased in a dose-dependent manner when cells were stimulated with OSM (P<0.01) and the effect of OSM (50 ng/ml) was almost equal to the effect of IL-1 (Fig. 1A). However, OSM had no effect on the expression levels of MIP1α and RANTES (Fig. 1B and C).

OSM stimulates the progression of osteoblasts. Cells were stimulated with different concentrations of OSM (10, 30 and 50 ng/ml) for 24 h. An MTT assay was performed to detect cell viability, a wound healing assay was conducted to measure cell migration and a Transwell assay was employed to assess cell invasion. The results revealed that there were dose-dependent increases in cell viability, wound healing and cell invasion in the OSM groups compared with the control group (all P<0.01; Fig. 2). Following treatment with 10, 30 and 50 ng/ml OSM, cell viability increased 44, 75 and 91%, respectively (Fig. 2A). The wound healing area increased 94, 123 and 158% respectively, following treatment with 10, 30 and 50 ng/ml OSM (Fig. 2B). Cell invasion ability increased 480, 590 and 660% of the control, respectively (P<0.01; Fig. 2C).

The transfection efficiency of MCP-1siRNA in osteoblasts. To further verify that the stimulating effect of OSM on osteoblast progression was associated with MCP-1, MCP-1 mRNA levels were measured following the treatment of cells with OSM. Interference efficiency was identified by RT-qPCR and western blotting, which detected the mRNA and protein levels of MCP-1, respectively. The results demonstrated that the mRNA and protein levels of MCP-1were significantly increased in the OSM group, compared with the control group (P<0.01; Fig. 3). However, the mRNA and protein levels of MCP-1 were decreased in the OSM+siMCP-1 group compared with the OSM+mock group and similar to the OSM group (P<0.01; Fig. 3). These results demonstrated that transfection with siMCP-1 significantly decreased MCP-1 expression.

Effect of MCP-1 silencing on OSM-induced cell progression. To verify the effect of MCP-1 silencing on OSM-induced cell progression, an MTT assay was performed to measure cell viability, a wound healing assay was used to measure cell migration ability and a Transwell invasion assay was used to determine cell invasion. The results demonstrated that cell viability, wound healing area and cell invasion were significantly increased in the OSM group compared with the control group (all P<0.01) and significantly decreased in the OSM+siMCP-1 group compared with the OSM+mock group (all P<0.01; Fig. 4). Cell viability, migration and invasion were similar in the OSM+mock and OSM groups. Cell viability increased 73% in the OSM group, compared with the control, while cell viability decreased 33% in the OSM+siMCP-1 group, compared with the OSM group (Fig. 4A). The wound healing area increased 111% in the OSM group, compared with the control, while that of OSM + siMCP-1 group decreased 44% compared with the OSM group (Fig. 4B). Cell invasion activity of the OSM group increased 610%, compared with the control, whereas that of the OSM+siMCP-1 group decreased 77%, compared with the OSM group, a little higher compared with the control group (P<0.01; Fig. 4C).

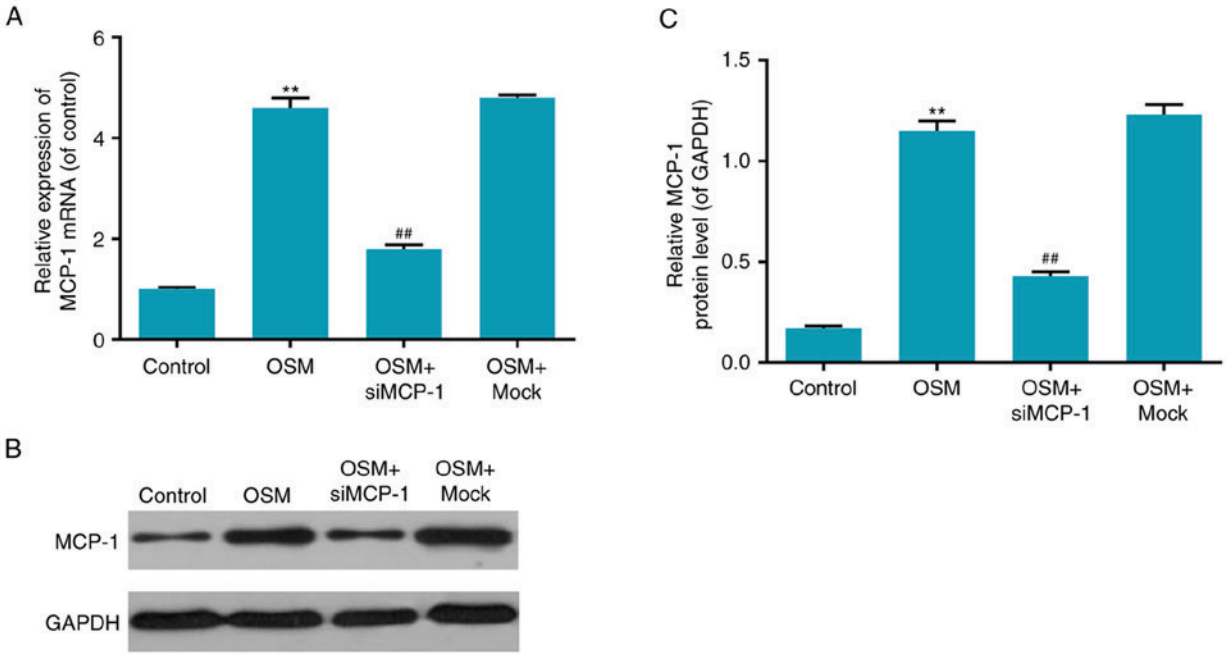

Figure 3. The silencing effect of siMCP-1 in OSM stimulated osteoblasts was determined. (A) The silencing effect of siMCP-1 was detected by reverse transcription-quantitative polymerase chain reaction following siMCP-1 transfection and/or OSM stimulation (B and C) The silencing effect of siMCP-1 was detected by western blotting following siMCP-1 transfection and/or OSM stimulation. GAPDH was used as a loading control. Data are presented as the mean ± standard deviation n=5. **P<0.01 vs. control and $^{\#\#}$P<0.01 vs. OSM+mock. OSM+siMCP-1 group, group transfected with siMCP-1 and treated with 30 ng/ml OSM; OSM+mock group, group transfected with non-specific siRNA and treated with 30 ng/ml OSM; OSM group, control group treated with 30 ng/ml OSM; control group, control group that received no treatment; OSM, oncostatin M; MCP-1, monocyte chemotactic protein-1; si, small interfering.

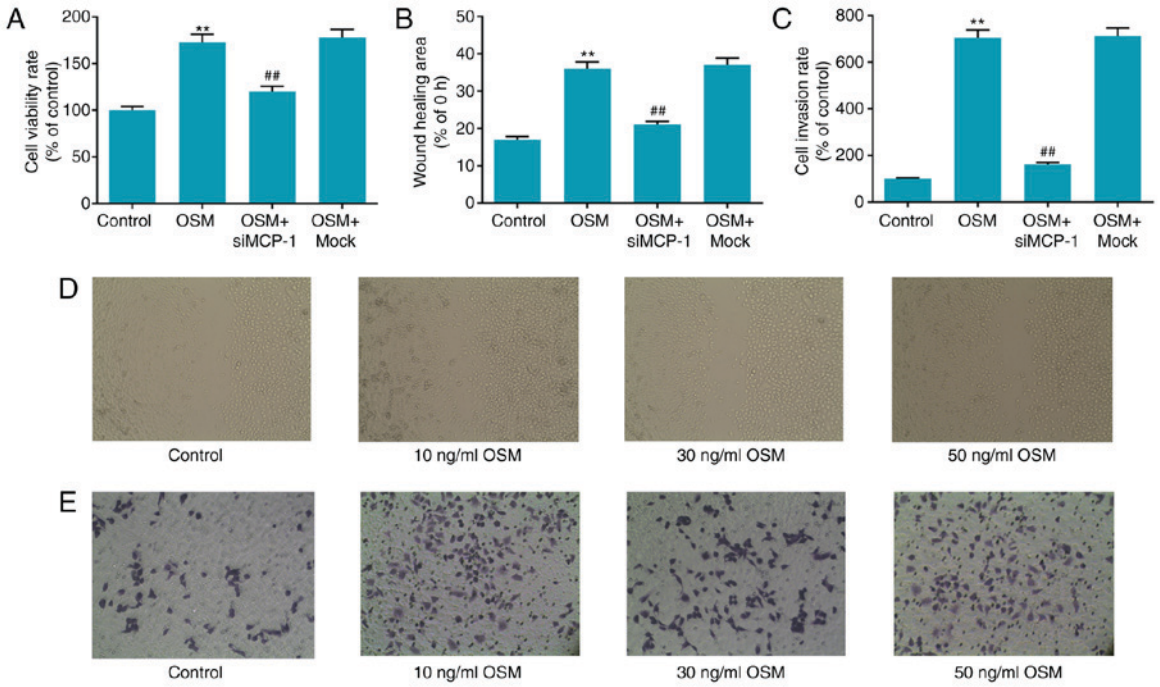

Figure 4. Effect of MCP-1 silencing on OSM induced cell progression. (A) An MTT assay was performed to detect cell viability and cells were counted 24 h following stimulation with OSM (30 ng/ml). (B) Cell migration was measured by performing a wound healing assay. (C) Cell invasion abilities were evaluated by performing a Transwell invasion assay and cells were counted following 24 h incubation. Images of (D) wound healing assay and (E) Transwell invasion assay, magnification x200. Data were presented as the mean ± standard deviation n=5. **P<0.01 vs. control and $^{\#\#}$P<0.01 vs. OSM+mock. OSM+siMCP-1 group, group transfected with siMCP-1 and treated with 30 ng/ml OSM; OSM+mock group, group transfected with non-specific siRNA and treated with 30 ng/ml OSM; OSM group, control group treated with 30 ng/ml OSM; control group, control group that received no treatment; MCP-1, monocyte chemotactic protein-1; OSM, oncostatin M; si, small interfering.

MCP-1-mediated OSM promotes the phosphorylation of protein kinase B (Akt). To assess whether MCP-1 is associated with the regulation of OSM on Akt phosphorylation in osteoblasts, western blot analysis was performed. The results

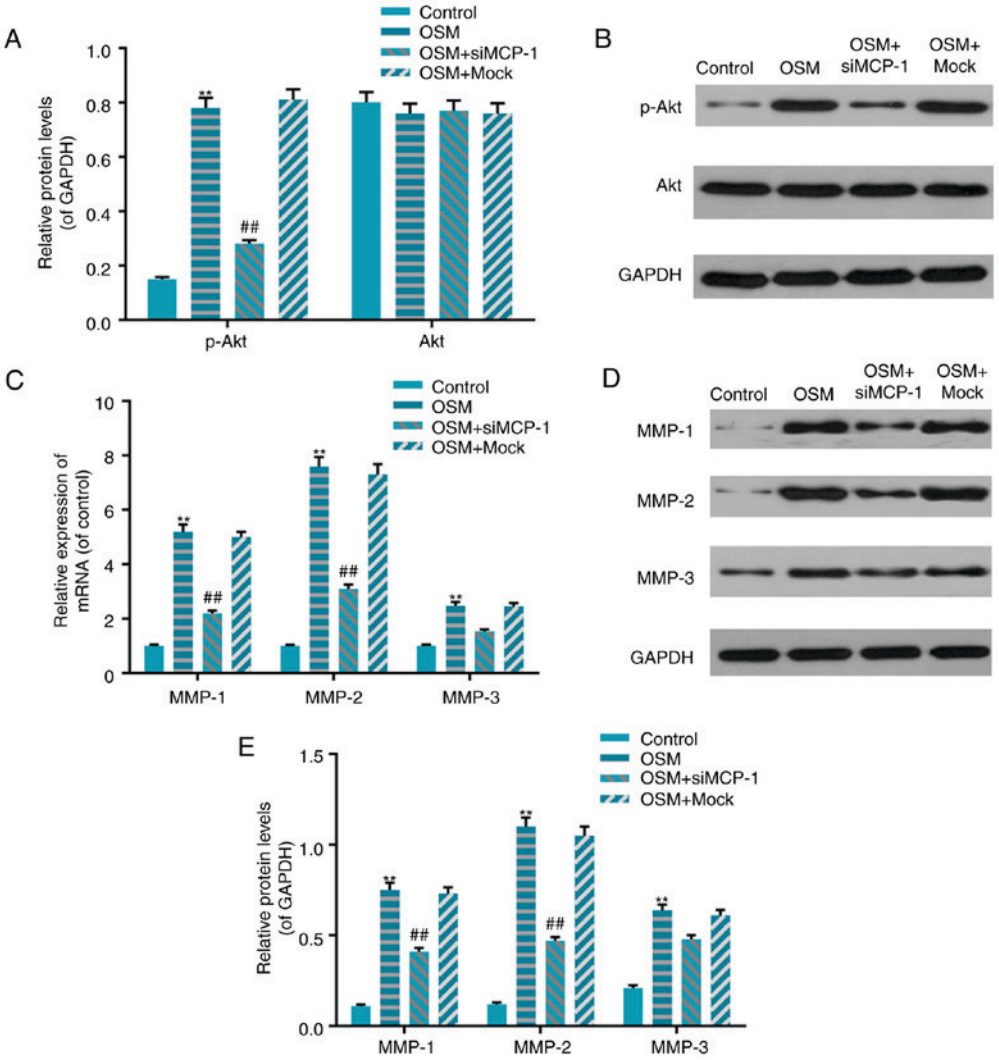

Figure 5. MCP-1 mediated OSM regulated Akt phosphorylation and MMP expression. (A and B) MCP-1 mediated OSM-stimulated Akt phosphorylation. Western blotting was performed to measure the phosphorylation of Akt. (C, D and E) MCP-1 mediated OSM regulated the expression of MMPs. (C) Reverse transcription-quantitative polymerase chain reaction and (D and E) western blotting were performed. Data were presented as the mean ± standard deviation. n=5. **P<0.01 vs. control and $^{\#\#}$P<0.01 vs. OSM+mock. OSM+siMCP-1 group, group transfected with siMCP-1 and treated with 30 ng/ml OSM; OSM+mock group, group transfected with non-specific siRNA and treated with 30 ng/ml OSM; OSM group, control group treated with 30 ng/ml OSM; control group, control group that received no treatment; MCP-1, monocyte chemotactic protein-1; OSM, oncostatin M; Akt, protein kinase B; MMP, matrix metalloproteinase; si, small interfering.

demonstrated that OSM significantly enhanced Akt phosphorylation levels compared with the control (P<0.01) and that these effects were partially blocked following siMCP-1 transfection (P<0.01; Fig. 5A). The phosphorylation levels of Akt in the OSM+siMCO-1 group decreased by 66% compared with the OSM+mock group (P<0.01; Fig. 5A and B).

MCP-1-mediated OSM regulates MMP production. To further clarify the underlying mechanism of invasion activity induced by OSM, levels of MMP-1, MMP-2 and MMP-3 mRNA and protein were measured in the siMCP-1+OSM groups. The results demonstrated that OSM significantly increased MMP-1, MMP-2 and MMP-3 mRNA and protein levels compared with the control (P<0.01; Fig. 5C-E). However, these effects were partially blocked by siMCP-1 transfection; MMP-1 and MMP-2 levels were significantly decreased in the OSM+siMCP-1 group compared with the OSM+mock group (P<0.01; Fig. 5C-E). Although transfection with siMCP-1 decreased the mRNA and protein levels of MMP-3, compared with the group that underwent treatment with OSM, this decrease was not significant (Fig. 5C-E).

Discussion

Skeletal repair and remodeling throughout life are essential to maintain bone integrity. Cytokines and chemokines are important factors that regulate cell recruitment during activation of the bone remodeling process. Although increasing attention has been given to the role of OSM during osteoblast development, it remains unknown whether OSM is associated with MCP-1during this process. Therefore, the present study was performed to determine the underlying molecular mechanisms of OSM on MCP-1 during osteoblast activity.

The activation and resorption of the bone matrix, and the formation of new bones are processes that occur during the bone remodeling process (31). Chemokines are small proteins weighing 8-10 kDa, which serve important roles in host defense systems and help to maintain normal tissues status (32,33).

Therefore, the present study determined the effects of different cytokines, including OSM, IL-1, IL-6, IL-11 and LIF on the expression of different chemokines, including MCP-1, MIP1α and RANTES. The results suggested that OSM stimulated MCP-1 production in a dose-dependent manner and that the effect of 50 ng/ml OSM on MCP-1 was almost equal to that of 10 ng/ml IL-1, which has been previously reported to stimulate chemokine activity (34,35). MIP1α directly stimulates osteoclast production and RANTES induces osteoclast differentiation (36). However, the results of the current study demonstrated that only IL-1 upregulated the expression of MIP1α and RANTES. Although elevated IL-6 and LIF levels have been reported in patients with rheumatoid arthritis, IL factors, such as IL-6, LIF and IL-11 did not stimulate the production of MCP-1, MIP1α and RANTES in the present study. This may be due to the fact that osteoblasts exhibit low levels of IL-6, LIF and IL-11 receptors (37).

The present study subsequently verified whether OSM induces the progression of osteoblasts in a dose-dependent manner. The effects of OSM (10, 30 and 50 ng/ml) on the viability, migration and invasion of osteoblasts were assessed. Following the silencing of MCP-1 expression by siRNA, the expression of MCP-1 mRNA and protein were not increased in osteoblasts following treatment with OSM and neither were osteoblast viability, migration and invasion. This suggests that MCP-1 mediates the stimulatory action of OSM in osteoblasts. In addition, cell signaling activated by OSM in osteoblasts maybe associated with Akt phosphorylation. The phosphatidylinositol-3-kinase/Akt signaling pathway serves an important role in cell proliferation, differentiation and apoptosis. Mice that have experienced Akt gene knockout grow slowly and exhibit signs of osteoporosis, including the increased apoptosis of osteoblasts (38). By contrast, the activation of Akt signaling in mature osteoblasts may inhibit apoptosis and prolong the life of osteoblasts (39). The results of the current study revealed that the phosphorylation of Akt was increased in osteoblasts treated with OSM; however, this increase was attenuated by MCP-1 silencing. This indicates that OSM activates Akt in osteoblasts via MCP-1, which may, in turn stimulate cell proliferation.

MMPs exist in the bone matrix and are proteases that degrade collagens, regulate the proteolysis of extracellular matrix structural proteins and induce cell metastasis (40,41). MMP-2 is secreted by osteoblasts and initiates bone reabsorption and formation by degrading the bone matrix, acting as the coupling factor that co-regulates bone reabsorption and bone formation (42,43). It has been demonstrated that levels of MMP-1 and MMP-3 are elevated in rheumatoid synovial fibroblasts (44). In the present study, levels of MMP-1, -2 and -3 were elevated in cells treated with OSM. Following transfection with siMCP-1, the pathway was blocked and the levels of MMP-1 and MMP-2 decreased. Levels of MMP-3 also decreased following transfection, although this decrease was not significant. This suggests that OSM treatment primarily affects MMP-1 (collagenases) and MMP-2 (gelatinases) in osteoblasts but has a smaller effect on MMP-3 (stromelysin). Furthermore, these results indicate that this process is mediated by MCP-1.

In conclusion, the results of the present study demonstrated that OSM affects the viability, migration and invasion of osteoblasts. These effects may be mediated by MCP-1, which regulate levels of phosphorylated Akt and the activation of MMP-1 and MMP-2. The results of the current study may provide novel insights and targets for skeletal repair and remodeling in clinical applications.

Acknowledgements

Not applicable.

Funding

Not applicable.

Availability of data and materials

All data generated or analyzed during this study are included in this published article.

Authors' contributions

JG conceived the study and WB performed the experiments.

Ethics approval and consent to participate

Not applicable.

Patient consent for publication

Not applicable.

Competing interests

The authors declare that they have no competing interests.

References

1. Michalski MN and McCauley LK: Macrophages and skeletal health. Pharmacol Ther 174: 43-54, 2017.
2. Holliday LS, McHugh KP, Zuo J, Aguirre JI, Neubert JK and Rody WJ Jr.: Exosomes: Novel regulators of bone remodelling and potential therapeutic agents for orthodontics. Orthod Craniofac Res 20 (Suppl 1): S95-S99, 2017.
3. Iqbal J, Yuen T, Kim SM and Zaidi M: Opening windows for bone remodeling through a SLIT. J Clin Invest 128: 1255-1257, 2018.
4. Boucher E, Marin M, Holani R, Young-Speirs M, Moore DM and Cobo ER: Characteristic pro-inflammatory cytokines and host defence cathelicidin peptide produced by human monocyte-derived macrophages infected with Neospora caninum. Parasitology: 1-14, 2017.
5. Mishra N, Mohata M, Aggarwal H, Chaudhary O, Das BK, Sinha S, Hazarika A and Luthra K: Expression of complement receptor 3 (CR3) and regulatory protein CD46 on dendritic cells of antiretroviral naive and treated HIV-1 infected individuals: Correlation with immune activation status. Mol Immunol 96: 83-87, 2018.
6. Sheikh V, Kasapoglu P, Zamani A, Basiri Z, Tahamoli-Roudsari A and Alahgholi-Hajibehzad M: Vitamin D3 inhibits the proliferation of T helper cells, downregulate $CD4^+$ T cell cytokines and upregulate inhibitory markers. Hum Immunol 79: 439-445, 2018.
7. Yano S, Mentaverri R, Kanuparthi D, Bandyopadhyay S, Rivera A, Brown EM and Chattopadhyay N: Functional expression of beta-chemokine receptors in osteoblasts: role of regulated upon activation, normal T cell expressed and secreted (RANTES) in osteoblasts and regulation of its secretion by osteoblasts and osteoclasts. Endocrinology 146: 2324-2335, 2005.

8. Fuller K, Owens JM and Chambers TJ: Macrophage inflammatory protein-1 alpha and IL-8 stimulate the motility but suppress the resorption of isolated rat osteoclasts. J Immunol 154: 6065-6072, 1995.
9. Moreaux J, Hose D, Kassambara A, Reme T, Moine P, Requirand G, Goldschmidt H and Klein B: Osteoclast-gene expression profiling reveals osteoclast-derived CCR2 chemokines promoting myeloma cell migration. Blood 117: 1280-1290, 2011.
10. Palmqvist P, Persson E, Conaway HH and Lerner UH: IL-6, leukemia inhibitory factor and oncostatin M stimulate bone resorption and regulate the expression of receptor activator of NF-kappa B ligand, osteoprotegerin and receptor activator of NF-kappa B in mouse calvariae. J Immunol 169: 3353-3362, 2002.
11. Yang WH, Tsai CH, Fong YC, Huang YL, Wang SJ, Chang YS and Tang CH: Leptin induces oncostatin M production in osteoblasts by downregulating miR-93 through the Akt signaling pathway. Int J Mol Sci 15: 15778-15790, 2014.
12. Richards CD, Langdon C, Deschamps P, Pennica D and Shaughnessy SG: Stimulation of osteoclast differentiation in vitro by mouse oncostatin M, leukaemia inhibitory factor, cardiotrophin-1 and interleukin 6: Synergy with dexamethasone. Cytokine 12: 613-621, 2000.
13. Walker EC, McGregor NE, Poulton IJ, Solano M, Pompolo S, Fernandes TJ, Constable MJ, Nicholson GC, Zhang JG, Nicola NA, *et al*: Oncostatin M promotes bone formation independently of resorption when signaling through leukemia inhibitory factor receptor in mice. J Clin Invest 120: 582-592, 2010.
14. Kakutani Y, Shioi A, Shoji T, Okazaki H, Koyama H, Emoto M and Inaba M: Oncostatin M promotes osteoblastic differentiation of human vascular smooth muscle cells through JAK3-STAT3 pathway. J Cell Biochem 116: 1325-1333, 2015.
15. Chen CY, Su CM, Huang YL, Tsai CH, Fuh LJ and Tang CH: CCN1 induces oncostatin M production in osteoblasts via integrin-dependent signal pathways. PLoS One 9: e106632, 2014.
16. Sarkozi R, Corazza U, Osterkamp JP, Pirklbauer M, Mayer G and Schramek H: Synergistic induction of CCL2/MCP-1 expression driven by oncostatin M and IL-1β in human proximal tubular cells depends on STAT3 and p65 NFκB/RelA. Physiol Rep 3: e12298, 2015.
17. Schnittker D, Kwofie K, Ashkar A, Trigatti B and Richards CD: Oncostatin M and TLR-4 ligand synergize to induce MCP-1, IL-6 and VEGF in human aortic adventitial fibroblasts and smooth muscle cells. Mediators Inflamm 2013: 317503, 2013.
18. Pasquier J, Gosset M, Geyl C, Hoarau-Vechot J, Chevrot A, Pocard M, Mirshahi M, Lis R, Rafii A and Touboul C: CCL2/CCL5 secreted by the stroma induce IL-6/PYK2 dependent chemoresistance in ovarian cancer. Mol Cancer 17: 47, 2018.
19. Polacchini A, Girardi D, Falco A, Zanotta N, Comar M, De Carlo NA and Tongiorgi E: Distinct CCL2, CCL5, CCL11, CCL27, IL-17, IL-6, BDNF serum profiles correlate to different job-stress outcomes. Neurobiol Stress 8: 82-91, 2018.
20. Garcia-Velasco JA, Seli E and Arici A: Regulation of monocyte chemotactic protein-1 expression in human endometrial stromal cells by integrin-dependent cell adhesion. Biol Reprod 61: 548-552, 1999.
21. Lisignoli G, Piacentini A, Cristino S, Grassi F, Cavallo C, Cattini L, Tonnarelli B, Manferdini C and Facchini A: CCL20 chemokine induces both osteoblast proliferation and osteoclast differentiation: Increased levels of CCL20 are expressed in subchondral bone tissue of rheumatoid arthritis patients. J Cell Physiol 210: 798-806, 2007.
22. Bojic S, Kotur-Stevuljevic J, Aleksic A, Gacic J, Memon L and Simic-Ogrizovic S: Matrix metalloproteinase-9 and tissue inhibitor of matrix metalloproteinase-1 in sepsis after major abdominal surgery. Dis Markers 2018: 5064684, 2018.
23. Gershtein ES, Mushtenko SV, Ermilova VD, Levchenko NE and Kushlinskii NE: Matrix metalloproteinases and their tissue inhibitors in blood serum of patients with endometrial cancer: Clinical and morphological correlations. Bull Exp Biol Med 165: 75-79, 2018.
24. Paiva KBS and Granjeiro JM: Matrix metalloproteinases in bone resorption, remodeling and repair. Prog Mol Biol Transl Sci 148: 203-303, 2017.
25. Clark IM, Powell LK, Ramsey S, Hazleman BL and Cawston TE: The measurement of collagenase, tissue inhibitor of metalloproteinases (TIMP) and collagenase-TIMP complex in synovial fluids from patients with osteoarthritis and rheumatoid arthritis. Arthritis Rheum 36: 372-379, 1993.
26. Walakovits LA, Moore VL, Bhardwaj N, Gallick GS and Lark MW: Detection of stromelysin and collagenase in synovial fluid from patients with rheumatoid arthritis and posttraumatic knee injury. Arthritis Rheum 35: 35-42, 1992.
27. Jablonska-Trypuc A, Matejczyk M and Rosochacki S: Matrix metalloproteinases (MMPs), the main extracellular matrix (ECM) enzymes in collagen degradation, as a target for anticancer drugs. J Enzyme Inhib Med Chem 31 (Sup 1): S177-S183, 2016.
28. Fan X, Hughes BG, Ali MA, Chan BY, Launier K and Schulz R: Matrix metalloproteinase-2 in oncostatin M-induced sarcomere degeneration in cardiomyocytes. Am J Physiol Heart Circ Physiol 311: H183-H189, 2016.
29. Ko HS, Park BJ, Choi SK, Kang HK, Kim A, Kim HS, Park IY and Shin JC: STAT3 and ERK signaling pathways are implicated in the invasion activity by oncostatin M through induction of matrix metalloproteinases 2 and 9. Yonsei Med J 57: 761-768, 2016.
30. Livak KJ and Schmittgen TD: Analysis of relative gene expression data using real-time quantitative PCR and the 2(-Delta Delta C(T)) method. Methods 25: 402-408, 2001.
31. Komar HM, Hart PA, Cruz-Monserrate Z, Conwell DL and Lesinski GB: Local and systemic expression of immunomodulatory factors in chronic pancreatitis. Pancreas 46: 986-993, 2017.
32. Wehmeyer C, Pap T, Buckley CD and Naylor AJ: The role of stromal cells in inflammatory bone loss. Clin Exp Immunol 189: 1-11, 2017.
33. Bozec A and Zaiss MM: T regulatory cells in bone remodelling. Curr Osteoporos Rep 15: 121-125, 2017.
34. Tian DS, Peng J, Murugan M, Feng LJ, Liu JL, Eyo UB, Zhou LJ, Mogilevsky R, Wang W and Wu LJ: Chemokine CCL2-CCR2 signaling induces neuronal cell death via STAT3 activation and IL-1β production after status epilepticus. J Neurosci 37: 7878-7892, 2017.
35. Bauer D, Redmon N, Mazzio E and Soliman KF: Apigenin inhibits TNFα/IL-1α-induced CCL2 release through IKBK-epsilon signaling in MDA-MB-231 human breast cancer cells. PloS One 12: e0175558, 2017.
36. de Jager SC, Bongaerts BW, Weber M, Kraaijeveld AO, Rousch M, Dimmeler S, van Dieijen-Visser MP, Cleutjens KB, Nelemans PJ, van Berkel TJ, *et al*: Chemokines CCL3/MIP1α, CCL5/RANTES and CCL18/PARC are independent risk predictors of short-term mortality in patients with acute coronary syndromes. PLoS One 7: e45804, 2012.
37. Amarasekara DS, Yun H, Kim S, Lee N, Kim H and Rho J: Regulation of osteoclast differentiation by cytokine networks. Immune Netw 18: e8, 2018.
38. Kawamura N, Kugimiya F, Oshima Y, Ohba S, Ikeda T, Saito T, Shinoda Y, Kawasaki Y, Ogata N, Hoshi K, *et al*: Akt1 in osteoblasts and osteoclasts controls bone remodeling. PLoS One 2: e1058, 2007.
39. Yang G, Sun Q, Teng Y, Li F, Weng T and Yang X: PTEN deficiency causes dyschondroplasia in mice by enhanced hypoxia-inducible factor 1alpha signaling and endoplasmic reticulum stress. Development 135: 3587-3597, 2008.
40. Yang Y, Li X, Du J, Yin Y and Li Y: Involvement of microRNAs-MMPs-E-cadherin in the migration and invasion of gastric cancer cells infected with Helicobacter pylori. Exp Cell Res 367: 196-204, 2018.
41. Filanti C, Dickson GR, Di Martino D, Ulivi V, Sanguineti C, Romano P, Palermo C and Manduca P: The expression of metalloproteinase-2, -9 and -14 and of tissue inhibitors-1 and -2 is developmentally modulated during osteogenesis in vitro, the mature osteoblastic phenotype expressing metalloproteinase-14. J Bone Min Res 15: 2154-2168, 2000.
42. Slompo C, Buzalaf CP, Damante CA, Martins GM, Hannas AR, Buzalaf MA and Oliveira RC: Fluoride modulates preosteoblasts viability and matrix metalloproteinases-2 and -9 activities. Braz Dent J 23: 629-634, 2012.
43. Leung K: ^{123}I-c(RGDfK)-human serum albumin-tissue inhibitor of matrix metalloproteinase 2 fusion protein: Molecular Imaging and Contrast Agent Database (MICAD). National Center for Biotechnology Information (US), Bethesda (MD), 2004.
44. Hanabayashi M, Takahashi N, Sobue Y, Hirabara S, Ishiguro N and Kojima T: Hyaluronan oligosaccharides induce MMP-1 and -3 via transcriptional activation of NF-κB and p38 MAPK in rheumatoid synovial fibroblasts. PLoS One 11: e0161875, 2016.